Renormalization group for scaling at the torus-doubling terminal point

Sergey Kuznetsov, Ulrike Feudel, and Arkady Pikovsky
Institute for Theoretical Physics and Astrophysics, University of Potsdam, Am Neuen Palais, Postfach 601553, D-14415 Potsdam, Germany
(Received 21 February 1997)

The quasiperiodically forced logistic map is analyzed at the terminal point of the torus-doubling bifurcation curve, where the dynamical regimes of torus, doubled torus, strange nonchaotic attractor, and chaos meet. Using the renormalization group approach we reveal scaling properties both for the critical attractor and for the parameter plane topography near the critical point. [S1063-651X(98)11002-4]

PACS number(s): 05.45.+b

I. INTRODUCTION

The transition from regular to chaotic dynamics via quasiperiodicity has attracted great interest. Starting from the seminal works of Landau [1] and Ruelle and Takens [2], different aspects of this transition have been studied both theoretically and experimentally. Some subtle details of quasiperiodic dynamics do not manifest themselves in a straightforward way in autonomous systems, but can be considered and understood for systems under quasiperiodic external force. Indeed, in the autonomous case the basic frequencies are determined by the internal dynamics. Contrary to this, in quasiperiodically forced systems the frequencies of the forcing can be taken arbitrary and kept independent from the dynamics. Recently, it has been found that the transition to chaos in quasiperiodically forced systems is generally mediated by strange nonchaotic attractors (SNA); this makes the whole picture highly nontrivial.

The SNAs were first described by Grebogi *et al.* in 1984 [3] and since then they have been investigated in a number of numerical [4–17] and experimental [18,19] studies. SNAs exhibit some properties of regular as well as chaotic regimes. Like regular attractors, they have only negative Lyapunov exponents (besides the zero exponent, connected to the phase variables of the quasiperiodic forcing); as for usual chaotic attractors their geometric structure is fractal-like. Also, their correlation properties lie between order and chaos: as shown in [14,20], they can generate a singular continuous spectrum. It is noteworthy that SNAs appear in studies of spectra and eigenfunctions of quantum systems with a quasiperiodic potential [4,21,22]. Mathematical research on SNA is still in the beginning phase [23,24].

In this paper we study the dynamics of the quasiperiodically forced logistic map [25–28,10,17]. It is known that this model demonstrates rich dynamical behavior, in particular, quasiperiodicity, torus-doubling bifurcations, SNA, and chaos. We focus our attention on one particular point in the parameter plane of the forced logistic map, the torus-doubling terminal point (TDT). This critical point is of crucial importance for understanding the entire picture of the dynamics because the regimes of quasiperiodic motion, SNA, and chaos meet at this point. To describe the dynamics at this critical point we develop the renormalization group (RG) approach. It allows one to examine the scaling properties of the critical attractor and to reveal the self-similar structure of the parameter plane topography near the TDT point.

II. THE MODEL AND BASIC REGIMES

Our basic model is the forced logistic map,

$$x_{t+1}=\lambda-x_t^2+\varepsilon\cos(2\pi\omega t+\phi),\quad \omega=(\sqrt{5}-1)/2,\quad (1)$$

where ε and ω are the amplitude and the irrational frequency of the forcing. Alternatively, we can rewrite it as a two-dimensional skew system:

$$\begin{aligned} x_{t+1}&=\lambda-x_t^2+\varepsilon\cos(2\pi y_t)\equiv f(x_t,y_t),\\ y_{t+1}&=y_t+\omega \pmod 1. \end{aligned}\quad (2)$$

In this formulation the parameter ϕ corresponds to the initial value of y: $2\pi y_0=\phi$. Figure 1 illustrates the basic regimes observed in the model (1).

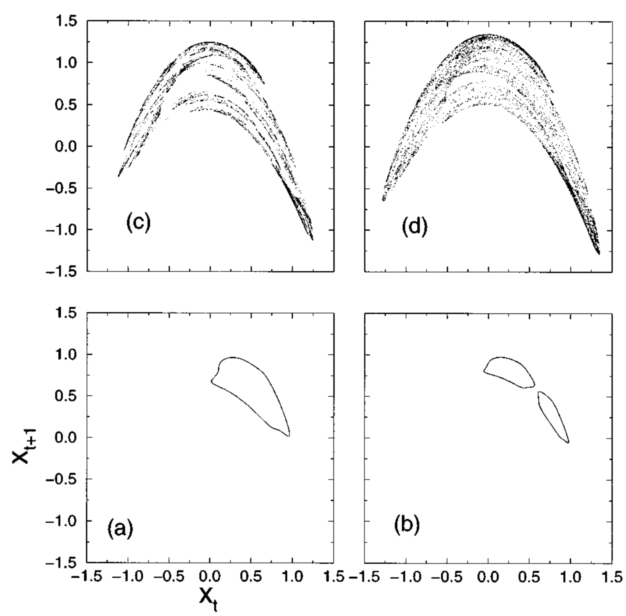

FIG. 1. The regimes in the system (1): (a) $T1$ for $\varepsilon=0.3$, $\lambda=0.9$; (b) $T2$ for $\varepsilon=0.15$, $\lambda=0.9$; (c) SNA for $\varepsilon=0.45$, $\lambda=0.8$; (d) C for $\varepsilon=0.45$, $\lambda=0.9$.

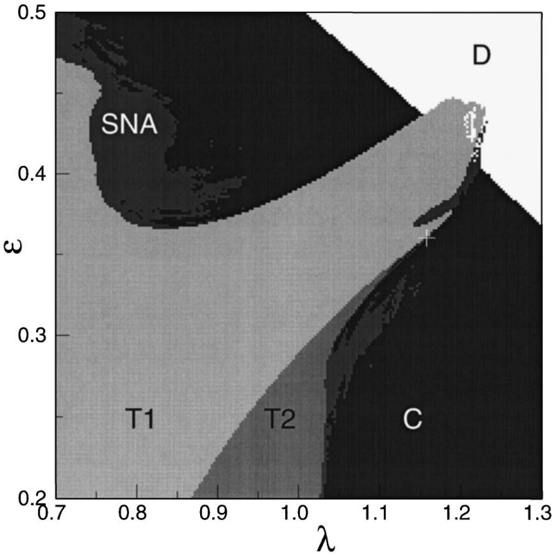

FIG. 2. Different regimes in the quasiperiodically forced logistic map, shown in a grey-scale code. From white to black: divergence (D), torus $(T1)$, doubled torus $(T2)$, strange nonchaotic attractor (SNA), chaos (C). The TDT $(\lambda\approx1.16,\ \varepsilon\approx0.36)$ point is marked with white cross.

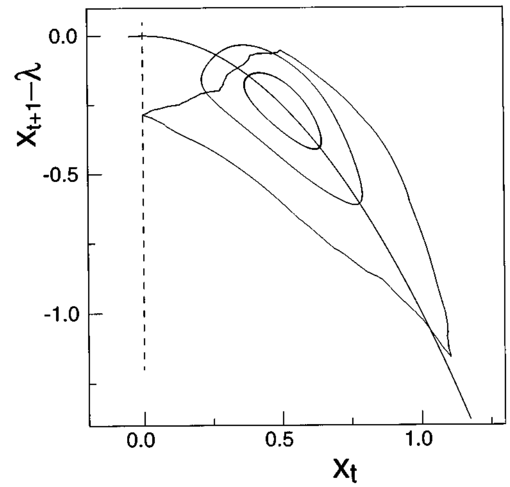

FIG. 3. The tori at the points of doubling: smooth tori for $\varepsilon=0.1,\ \lambda=0.778\,791$ and $\varepsilon=0.2,\ \lambda=0.824501$, and the critical torus for ε_c,λ_c. For visual clarity the vertical coordinate is shifted by λ so that the logistic map has the same form for all parameter values. The critical torus evidently touches the line $x_t=0$.

Consider first a value of the control parameter λ for which the unforced map $(\varepsilon=0)$ has a stable fixed point. Under small quasiperiodic forcing, the fixed point is transformed into a stable smooth invariant curve. Such curves appear in continuous-time dynamical systems as Poincaré mappings for the motion on a torus. Therefore with commonly used abuse of the terminology we call this curve the torus $T1$ [Fig. 1(a)]. If the force of small amplitude is applied to a stable period-2 orbit, it gives rise to an attractor consisting of two closed smooth curves, or the doubled torus $T2$ [Fig. 1(b)]. If we increase the forcing amplitude, it may happen that the smooth torus transforms into SNA [3,11]; the Lyapunov exponent remains negative, but the geometrical structure of the attractor becomes complex, fractal-like [Fig. 1(c)]. The regimes with a positive Lyapunov exponent can be classified as chaos (C); see Fig. 1(d). Finally, for large λ and ε a trajectory generated by the map (1) can escape to infinity, i.e., the divergence (D) takes place.

In Fig. 2 the regions of the regimes described above are depicted in the parameter plane (λ,ε). At each pixel the type of the regime was detected by analyzing the Lyapunov exponent and the phase sensitivity property [11]: tori: negative Lyapunov exponent without phase sensitivity; SNA: negative Lyapunov exponent with high phase sensitivity; chaos: positive Lyapunov exponent. In the diagram we see different transitions: $T1\leftrightarrow T2$, $T1\leftrightarrow$ SNA, etc. Some of these transitions are quite well understood [29,10,16], while the description of others is still incomplete. The subject of our main interest in this paper will be the "triple" point where the domains of tori $T1$ and $T2$, SNA, and chaos meet.

III. TORUS-DOUBLING CURVE AND ITS TERMINAL POINT

For zero amplitude $\varepsilon=0$ Eq. (1) becomes the usual logistic map and exhibits a cascade of period-doubling bifurcations. For finite but small amplitudes these bifurcations are transformed into torus-doubling bifurcations, at which an attractor consisting of 2^n curves splits into an attractor consisting of 2^{n+1} curves. The smaller the amplitude, the larger the number of the torus doublings seen with increasing λ; for any constant amplitude this number is finite [30,26]. The torus doubling have been observed numerically [29] and experimentally [31]; for mathematical background see [32].

In Fig. 2 one can see a curve in the parameter plane (λ,ε) where the first torus-doubling transition $T1\leftrightarrow T2$ occurs. This curve starts at the point $(3/4,0)$. For small amplitudes ε the attractor arisen from the fixed point of the logistic map is represented by a smooth invariant curve located entirely in the region $x>0$ (Fig. 3). Suppose that we increase the amplitude ε and go along the torus-doubling bifurcation curve in the parameter plane. Then, the torus becomes larger and larger, and the minimum value of x on it approaches zero. Finally, the attractor touches the line $x=0$, and this event corresponds, as we argue below, to the terminal point of the torus-doubling bifurcation curve, the TDT critical point. Indeed, as long as the torus occupies the region $x>0$, the mapping can be considered invertible, thus the mathematical theory [32] is applicable. As the torus touches the line $x=0$, the noninvertibility of the logistic map comes into play, and the torus doubling is destroyed. Another more constructive argument is based on rational approximations to the quasiperiodic forcing.

Let us consider the torus doubling in terms of rational approximants for the frequency ω. In our case of the reciprocal golden mean, these approximants are the ratios of Fibonacci numbers:

$$\omega_k=F_{k-1}/F_k,\quad k=1,2,\ldots,$$
$$F_0=0,\quad F_1=F_2=1,\quad F_{k+1}=F_k+F_{k-1}. \tag{3}$$

Instead of the $T1$ torus, for a rational frequency ω_k we get a cycle of period F_k. Increasing the control parameter λ we

TABLE I. Critical parameter values for the rational approximations.

ω_k	λ	ε	ϕ_c^k
2/3	0.893 135 90	0.390 455 26	2.388 140 31
3/5	1.076 332 88	0.305 114 53	2.270 929 15
8/13	1.140 773 98	0.356 371 73	2.474 385 70
13/21	1.134 538 32	0.353 262 66	2.517 043 66
34/55	1.155 871 57	0.360 212 07	2.483 410 89
55/89	1.153 649 97	0.358 649 70	2.471 294 47
144/233	1.157 906 81	0.360 223 44	2.482 951 10
233/377	1.157 207 06	0.359 951 20	2.485 317 55
610/987	1.158 075 55	0.360 246 55	2.483 280 49
987/1597	1.157 924 94	0.360 190 31	2.482 596 05
2584/4181	1.158 094 62	0.360 248 06	2.483 219 66
4181/6765	1.158 063 54	0.360 237 23	2.483 355 60
10946/17711	1.158 096 58	0.360 248 35	2.483 236 05

expect to see a bifurcation of this cycle at some parameter value that gives an approximation to the torus-doubling bifurcation. In fact, for the rational frequencies ω_k the bifurcation point will depend on the initial phase ϕ. We can speak on the torus-doubling bifurcation only if this dependence disappears asymptotically for $k \to \infty$ (i.e., the limit does not depend on the initial phase, cf. [33]). Certainly, this is the case for small amplitudes ε, and we may gradually increase the amplitude and trace the torus-doubling curve as long as possible.

Now we are going to formulate the condition that the doubling torus touches the line $x=0$ in terms of rational approximations. So we fix a rational frequency $\omega_k = F_{k-1}/F_k$ and find the values of λ and ε to satisfy the following conditions:

(1) For some initial phase ϕ_c^k there exists a period-F_k cycle starting from $x=0$ (meaning that the cycle is superstable, with zero multiplier), and the derivative $dx/d\phi|_{0,\phi_c^k}$ vanishes (this condition means that the approximate torus touches the line $x=0$).

(2) The minimal multiplier reached at some other initial phase ϕ_m^k is equal to -1, i.e., for this phase the period-F_k cycle is at the threshold of the period-doubling bifurcation (this condition means that the approximate torus undergoes a doubling).

Of course, the second condition may be true only for the approximants with odd denominators, therefore we numerically studied only such approximations. In Table I we summarize the data of the computations. Estimating the limit $k \to \infty$, we get the TDT point for the map (1):

$$\lambda_c = 1.158\,0968, \quad \varepsilon_c = 0.360\,2485, \quad \phi_c = 2.483\,23, \tag{4}$$

where $\phi_c = \lim_{k\to\infty} \phi_c^k$.

For a rational frequency ω_k, at the point from Table I we have simultaneously a superstable cycle for the phase ϕ_z^k and a cycle at the period-doubling bifurcation threshold for the phase ϕ_m^k. Obviously, by an infinitesimal shift of the parameters λ, ε from this point we can reach a situation when the cycle remains stable at one phase ϕ and becomes unstable at another one. This means that the system demonstrates a bifurcation depending on the phase of the external force. According to [11] this is a criterion of the presence of SNA. So, we conclude that a small perturbation of the attractor at TDT can lead to a SNA. Numerical analysis shows that chaotic states also exist in the neighborhood of the TDT point. To describe the dynamics at the critical point and in its vicinity, we develop renormalization group approach in the next section.

IV. RENORMALIZATION GROUP AT THE TORUS-DOUBLING TERMINAL POINT

As usual, in a construction of a renormalization transformation for the golden-mean quasiperiodic dynamics [34,35,13] the main idea is to represent the mapping (2) over F_{k+2} iteration steps through the mappings over F_{k+1} and F_k steps:

$$f^{F_{k+2}}(x,y) = f^{F_k}(f^{F_{k+1}}(x,y), y + F_{k+1}\omega). \tag{5}$$

Due to a known relation for the golden mean

$$y + F_k\omega = y - (-\omega)^k \mod 1, \tag{6}$$

we immediately see that the appropriate constant for renormalization of the variable y is given by $(-\omega)$; the corresponding factor for the variable x we denote as a. Substituting in Eq. (5) the scaled function

$$g_k(x,y) = a^k f^{F_k}(a^{-k}x, (-\omega)^k y) \tag{7}$$

we obtain the final renormalization transformation

$$g_{k+2}(x,y) = a^2 g_k(a^{-1} g_{k+1}(x/a, -\omega y), \omega^2 y + \omega). \tag{8}$$

To find the solution of the RG equation (8) associated with the TDT point we have used the following procedure. First, we have taken the mapping (2) at the critical point $(\lambda_c, \varepsilon_c)$ to define the pair of functions g_1, g_2 as an initial condition for the recurrent procedure (8). Second, we have observed numerically that with a suitable a the iterations of (8) converge to a period-3 cycle. Finally, this period-3 solution has been improved using a quasi-Newton method for a polynomial approximation of the function $g(x,y)$ (with odd and even powers for y, and only even powers for x). The resulting numerical value of the constant a is found to be $a = 1.582\,5935$. However, because of the period-3 nature of the solution, we have to use the following scaling factors to observe self-similarity: for time: $\tau = \omega^{-3} = 4.236\,06\ldots$; for y variable: $\beta = (-\omega)^{-3} = -4.236\,06\ldots$; for x variable: $\alpha = a^3 = 3.963\,76\ldots$.

To study scaling properties of the parameter plane near the TDT critical point we need to consider the evolution of small perturbations to the found period-3 solution under iterations of the RG transformation. Linearization of the RG transformation (8) near the period-3 solution leads to an eigenproblem that we have solved numerically. The eigenvalues were computed as eigenvalues of the corresponding finite matrix approximation based on the polynomial representation of $g_{1,2}$. The relevant eigenvalues are

$$\delta_1 = 10.5029\ldots, \quad \delta_2 = 5.1881\ldots. \tag{9}$$

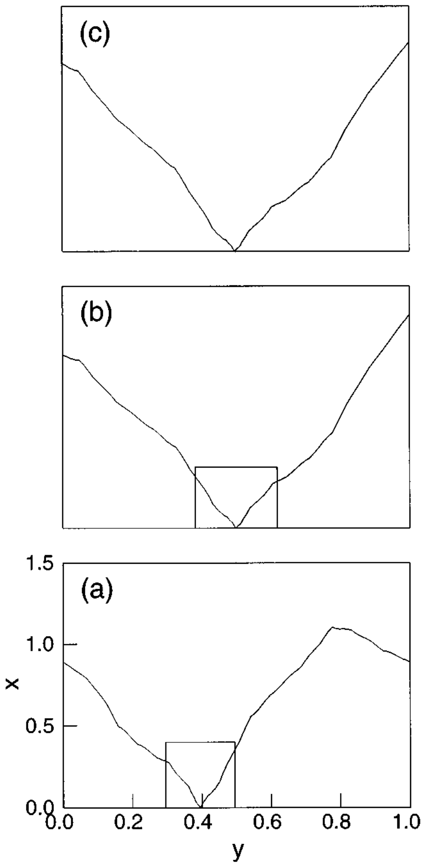

FIG. 4. Scaling of the critical torus. The whole torus is depicted in panel (a), the part in the box near the critical point $(0,y_c)$ is enlarged in panel (b). The central part of (b), magnified with the factors β along y and α along x is shown in panel (c).

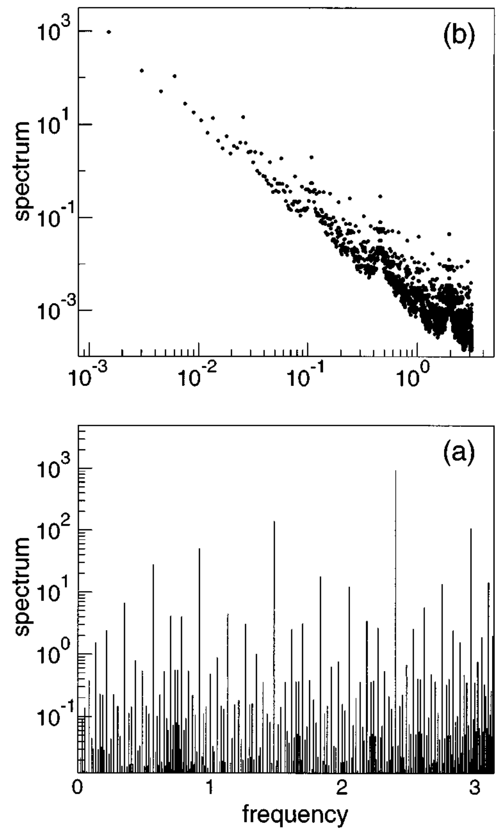

FIG. 5. Spectrum of the critical torus. (a) Spectrum of the process x_t. (b) Spectrum of the function $x(y)$.

Two other eigenvalues with modulus larger than 1 are present in the spectrum, $-3.963\ldots=-\alpha$ and $-4.236\ldots=\beta$, but they are not relevant: the first one corresponds to a perturbation pushing the iterations of Eq. (5) out of the class of commutative functional pairs; the second one corresponds to an infinitesimal shift of the origin for the y variable.

Let us define a coordinate system near the TDT critical point in the parameter plane in such a way that a shift along each coordinate axis gives rise to a perturbation associated with one eigenvalue, δ_1 or δ_2, respectively. In these *scaling coordinates* we expect to see a self-similar topography: the picture will reproduce itself under enlargement by the factors δ_1 and δ_2 along the coordinate axes. We check the predictions of the RG analysis in the next section.

V. SCALING AT THE TORUS-DOUBLING TERMINAL POINT AND ITS VICINITY

As we observed in Fig. 3, on the way along the torus-doubling bifurcation line towards the TDT point the attractor is represented by a smooth closed invariant curve. At the critical point it becomes a closed nonsmooth (fractal-like) curve and we call it the *critical torus*. In Fig. 4 the critical torus is presented as a graph in the coordinates (x,y). According to the RG analysis, the critical torus must demonstrate self-similarity on small scales near the point $x=0,y=y_c=\phi_c/2\pi$ and reproduce itself under enlargement with factors α and β along the axes x and y, respectively. In Figs. 4(b) and 4(c) we check this prediction.

From the stated scaling law it follows that at the point $x=0,y=y_c$ the critical torus has a singularity of the type

$$x\sim|y-y_c|^{\gamma},\qquad \gamma=\frac{\ln\alpha}{\ln\beta}=0.9539\ldots.$$

Occasionally, the power γ is close to one, therefore the singularity in the critical torus visually looks like a break. Note that due to ergodicity of the quasiperiodic rotation, the presence of a singularity at a single point means the presence of an infinite dense set of singularities on the critical torus. So, this is really a fractal object.

In Fig. 5 we present results of the spectral analysis for the critical torus. The panel (a) shows the usual Fourier spectrum for the time series x_n generated by the forced logistic map at the TDT point. This is just the spectrum that should be observed in experiment. The panel (b) presents a spectrum for the function $x(y)$ representing the form of the critical torus. This plot illustrates once more the fractal nature of the attractor: the amplitudes of spectral components are clearly seen to fall down according to a power law.

To illustrate scaling properties of the parameter plane topography near the TDT point of our model map (1) we need to define the scaling coordinates in the parameter plane

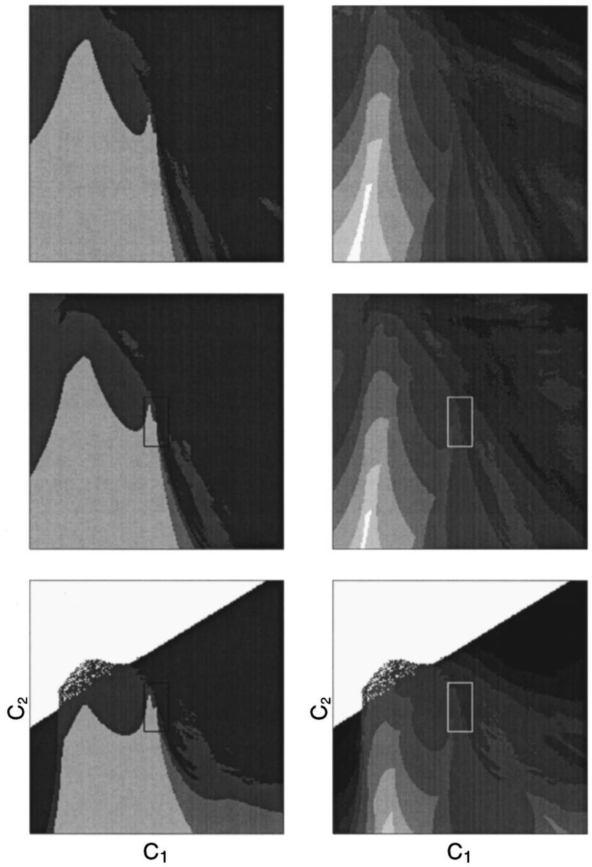

FIG. 6. Scaling in the vicinity of the critical point. Left column: different regimes grey-scale coded as in Fig. 2. Right column: the Lyapunov exponent coded in a grey scale. Bottom panel: a region around the TDT point (marked by white cross in Fig. 2) is shown in the coordinates C_1, C_2 (10). The small box is enlarged in the middle panel with the factors $\delta_{1,2}$, and the small box from the middle panel is enlarged in the top panel. The grey coding for the Lyapunov exponent is scaled with the factor τ.

(λ,ε). In fact, one coordinate axis corresponding to the leading eigenvalue δ_1 can be chosen almost arbitrarily, but the other coordinate direction should be carefully selected to exclude the contribution from the leading eigenvector. Numerically, we have found the following relations between the scaling coordinates C_1,C_2 and the parameters (λ,ε):

$$\varepsilon=\varepsilon_c-C_1+0.3347C_2, \quad \lambda=\lambda_c+C_2. \tag{10}$$

In Fig. 6 these coordinates are used to show the parameter plane arrangement around the critical point. One can see that the structure is indeed self-similar. This means that the regimes of torus, doubled torus, SNA, and chaos, that can be seen in panels (b) and (c), are present also in an arbitrary small vicinity of the TDT point.

VI. CONCLUSIONS

In this paper we have considered the dynamics of the quasiperiodically forced logistic map. Our particular point of interest was the torus-doubling terminal point. Around this point all relevant dynamical regimes (torus and doubled torus, strange nonchaotic attractor, and chaos) are present. The attractor at this point (''critical torus'') is represented by a fractal-like curve, its scaling properties are described with the renormalization group method. The RG approach developed in this paper allows us also to characterize the self-similar structure in the parameter plane near the torus-doubling terminal point.

The TDT point corresponds to a novel type of criticality for quasiperiodic dynamics at the onset of chaos, and the forced logistic map may be considered as a representative of the corresponding universality class. We conjecture that this class contains also the higher-dimensional systems such as the forced Hénon map. It would be interesting to observe this type of universal behavior in experiment. For this, one should take a nonlinear dissipative system demonstrating the period-doubling cascade, say, an electronic circuit with periodic driving (e.g., [36]), and apply an additional periodic force to have the proper irrational ratio of the frequencies. Then, the torus-doubling terminal point should be found, the critical torus with its fractal properties and the universal arrangement of the parameter space near the critical point should be observed.

The remarkable peculiarity of the presented analysis of the TDT critical point is that it links the problems of the quasiperiodic transition to chaos and strange nonchaotic attractors to the concepts of renormalization group, universality, and scaling. At the other known transitions to chaos, as in the circle map [34,35], there was no place for SNA. On the other hand, at the transition from a smooth torus to SNA analyzed in our previous work [13] there was no place for chaos. However, we see many open questions in the context of the undertaken research. What happens at other irrational frequencies? What can be said about the transitions $T\leftrightarrow$ SNA and SNA $\leftrightarrow$ chaos? Is it possible to develop a RG analysis for some other critical situations connected with birth or death of SNA? What does a generalization to higher-dimensional systems look like? We hope that the results of this paper will stimulate research in the directions outlined.

ACKNOWLEDGMENTS

We thank C. Grebogi, J. Kurths, and M. Zaks for valuable discussions. S.K. acknowledges support from the Max Planck Society and from the Russian Foundation of Fundamental Research (Project No. 97-02-16416).

[1] L. D. Landau, Dokl. Akad. Nauk SSSR **44**, 339 (1944).
[2] D. Ruelle and F. Takens, Commun. Math. Phys. **20**, 167 (1971).
[3] C. Grebogi, E. Ott, S. Pelikan, and J. A. Yorke, Physica D **13**, 261 (1984).
[4] A. Bondeson, E. Ott, and T. M. Antonsen, Phys. Rev. Lett. **55**, 2103 (1985).
[5] F. J. Romeiras *et al.*, Physica D **26**, 277 (1987).
[6] F. J. Romeiras and E. Ott, Phys. Rev. A **35**, 4404 (1987).
[7] M. Ding, C. Grebogi, and E. Ott, Phys. Rev. A **39**, 2593 (1989).
[8] M. Ding, C. Grebogi, and E. Ott, Phys. Lett. A **137**, 167 (1989).
[9] T. Kapitaniak, E. Ponce, and J. Wojewoda, J. Phys. A **23**, L383 (1990).
[10] J. F. Heagy and S. M. Hammel, Physica D **70**, 140 (1994).
[11] A. Pikovsky and U. Feudel, Chaos **5**, 253 (1995).
[12] U. Feudel, J. Kurths, and A. Pikovsky, Physica D **88**, 176 (1995).
[13] S. Kuznetsov, A. Pikovsky, and U. Feudel, Phys. Rev. E **51**, R1629 (1995).
[14] A. Pikovsky and U. Feudel, J. Phys. A **27**, 5209 (1994).
[15] M. Ding and J. Scott Kelso, Int. J. Bifurcation Chaos Appl. Sci. Eng. **4**, 553 (1994).
[16] Y.-C. Lai, Phys. Rev. E **53**, 57 (1996).
[17] T. Nishikawa and K. Kaneko, Phys. Rev. E **54**, 6114 (1996).
[18] W. L. Ditto *et al.*, Phys. Rev. Lett. **65**, 533 (1990).
[19] T. Zhou, F. Moss, and A. Bulsara, Phys. Rev. A **45**, 5394 (1992).
[20] U. Feudel, A. Pikovsky, and A. Politi, J. Phys. A **29**, 5297 (1996).
[21] J. A. Ketoja and I. I. Satija, Physica D **109**, 70 (1997).
[22] U. Feudel, A. S. Pikovsky, and M. A. Zaks, Phys. Rev. E **51**, 1762 (1995).
[23] G. Keller, Fundamenta Mathematicae **151**, 139 (1996).
[24] J. Stark, Physica D **109**, 163 (1997).
[25] K. Kaneko, Prog. Theor. Phys. **69**, 1806 (1983).
[26] S. P. Kuznetsov, Pisma Zh. Eksp. Teor. Fiz. **39**, 113 (1984) [JETP Lett. **39**, 113 (1984)].
[27] A. Arneodo, Phys. Rev. Lett. **53**, 1240 (1984).
[28] S. P. Kuznetsov and A. S. Pikovsky, Phys. Lett. A **140**, 166 (1989).
[29] K. Kaneko, *Collapse of Tori and Genesis of Chaos in Dissipative Systems* (World Scientific, Singapore, 1986).
[30] K. Kaneko, Prog. Theor. Phys. **69**, 1806 (1983).
[31] V. S. Anischenko, T. E. Letchford, and M. A. Safonova, Radiophysica **27**, 565 (1984).
[32] H. Broer, G. B. Huitema, F. Takens, and B. L. J. Braaksma, Mem. Amer. Math. Soc. **83**, 1 (1990).
[33] P. R. Chastell, P. A. Glendinning, and J. Stark, Phys. Lett. A **200**, 17 (1995).
[34] M. J. Feigenbaum, L. P. Kadanoff, and S. J. Shenker, Physica D **5**, 370 (1982).
[35] D. Rand, S. Ostlund, J. Sethna, and E. D. Siggia, Physica D **8**, 303 (1983).
[36] P. S. Linsay, Phys. Rev. Lett. **47**, 1349 (1981).